# Scenario-based Hybrid Model Predictive Design for Cooperative Adaptive Cruise Control in Mixed-autonomy Environments

Sahand Mosharafian, Yajie Bao, and Javad Mohammadpour Velni

Abstract—This paper presents a scenario-based hybrid model predictive control (MPC) design approach for cooperative adaptive cruise control (CACC) in mixed-autonomy traffic environments with uncertainties stemming from unexpected maneuvers of human-driven vehicles. Different from the past works that consider one possible realization of uncertainty, the proposed approach here considers multiple scenarios based on the uncertainty description that varies with the relative location of the human-driven vehicles (HVs) and the connected and automated vehicles (CAVs). For each scenario, a mixed integer quadratic programming problem is formulated for the control of CAVs with four operating modes, namely free following, braking, danger, and lane change. Each CAV's operating mode is determined based on the predictive information it receives from its predecessors and the anticipated behaviors of surrounding HVs. All the scenarios are handled simultaneously using the scenario-based MPC approach for a robust CACC. Simulations in a mixed-autonomy traffic system including two lanes demonstrate that the proposed scenario-based hybrid MPC approach significantly reduces deviations from the desired spacing policy and the desired velocity in the platoon during unexpected human-driven vehicle maneuvers, compared with the past work, particularly, a discrete hybrid stochastic (DHSA) MPC approach.

# I. INTRODUCTION

Lane change is a common driving maneuver. Inappropriate lane changes would result in fatal accidents. The acquisition of onboard sensor data and the information received through vehicle-to-vehicle (V2V) communication would improve safety and comfort during a lane-change maneuver [1]. Numerous researchers have concentrated on the problem of trajectory planning and control for a safe and efficient lane-change maneuver for autonomous vehicles [2]-[4]. In the existing literature, lane-change maneuvers have been investigated from different viewpoints, namely how an automated vehicle (AV) performs a collision-free lane change and how an AV or a platoon of CAVs react when an adjacent vehicle decides to change lane to robustify the traffic flow against lane-change maneuvers. Recently, in [5], the authors addressed the problem of robustifying CACC against HVs' maneuvers and maintaining the desired formation and spacing among vehicles in mixed autonomy traffic.

As demonstrated by our previous research study [5], integrating operating modes directly into the controller design yields optimal behavior of CAVs while considering

This work was financially supported by the US National Science Foundation under awards CNS-1931981 and CNS-2302215.

uncertainties in the environment. While the controller mainly focuses on maintaining the desired velocity and distance among CAVs, it may switch the CAV's operating mode to respond to an HV's random behavior. In our previous study, we optimized control inputs and the uncertainty variables simultaneously to minimize the control cost. However, in the case that optimized uncertainty variables do not match the realizations of uncertainties, the CAV cannot achieve its optimal performance. Hence, in this study, we aim to address the aforementioned issue using scenario-based model predictive control (SMPC). SMPC has been developed to account for system uncertainties for robust control design purposes by representing uncertainties using a scenario tree in the optimal control problem and reduce the conservativeness inherent to open-loop robust MPC by introducing recourse into optimal control problem [6]. The scenarios in the scenario tree can be generated by any model-based or data-driven approach. Moreover, online adaptive scenario generation has been proposed to reduce the conservativeness of scenario tree construction [7].

In this work, we propose to leverage the scenario trees to represent the uncertainties of the environments for MPC design, where the uncertainties can arise from unexpected maneuvers of human-driven vehicles. We incorporate the environment uncertainties represented by scenario trees into the structures of our previously proposed stochastic CACC approaches [5], [8]. In particular, we consider four operating modes including free following, braking, danger, and lane change to assure the desired performance while preserving safety in a mixed-traffic environment. To properly model the CAV's behaviors that include both continuous and binary variables, a hybrid mathematical model is required. We leverage the discrete hybrid automata to capture both continuous and binary variables. Finally, we present a scenario-based hybrid MPC as the optimal stochastic controller for each CAV. The operating mode of each CAV would be decided automatically depending on the status of the uncertainties that are captured through the scenario tree.

The contributions of the paper are as follows. This paper presents a scenario-based hybrid MPC design method for CACC in order to cope with the uncertainties in mixed-autonomy traffic environments. The controller allows to automatically switch between danger and lane-change modes, as well as adjust the steering angle to perform a lane-change maneuver when needed. The scenario tree allows the controller to capture possible realizations of uncertainties and thus robustify the CAV's performance against sudden changes in the environment caused by human-driven vehi-

S. Mosharafian and Y. Bao are with the School of Electrical & Computer Engineering, University of Georgia, Athens, GA 30602, USA. {sm50492, yb18054}@uga.edu.

J. Mohammadpour Velni is with Dept. of Mechanical Engineering, Clemson University, Clemson, SC 29634, USA. javadm@clemson.edu.

cles' maneuvers.

II. PROBLEM STATEMENT AND RELATED PRELIMINARIES Considering a CACC system with  $N_v$  CAVs,  $i \in \{0,1,\ldots,N_v-1\}$  denotes the  $i^{th}$  vehicle (CAV $_i$ ), and i=0 is the leader vehicle. CAVs' longitudinal and lateral movements are studied here where the goal of each CAV in the longitudinal movement is to reach a relatively small headway while preserving safety during sudden changes in the platoon, e.g., sudden deceleration or lane change performed by adjacent HVs. When an HV enters into the CAVs' platoon, CAVs may require a lane change to pass the interrupting HV and achieve their desired distance from their predecessor. Therefore, CAVs need to consider the uncertain maneuvers of HVs for robust and safe CACC.

Similar to [5], we consider the  $i^{th}$  vehicle's bicycle model as follows

$$\dot{\mathbf{X}}_{i}^{m}(t) = \begin{bmatrix} \dot{x}_{i}(t) \\ \dot{y}_{i}(t) \\ \dot{\theta}_{i}(t) \end{bmatrix} \approx \begin{bmatrix} v_{i}(t) \\ \theta_{i}(t) v_{i}(t_{0}) \\ u_{i}^{\varphi}(t) v_{i}(t_{0}) \end{bmatrix}, \tag{1}$$

where  $x_i$  and  $y_i$  indicate the vehicle's longitudinal and lateral location from a specified reference, respectively;  $\varphi_i$  is the steering angle,  $\theta_i$  is the vehicle's body angle with the X-axis,  $v_i$  is the vehicle's velocity, and the input  $u_i^{\varphi}$  denotes the steering rate. The distance between  $i^{th}$  vehicle and its preceding vehicle at time t is denoted by  $d_i(t)$  and defined as

$$d_i(t) = x_{i-1}(t) - x_i(t) - l_i^v, (2$$

where  $x_i$  and  $l_i^v$  are the longitude of the  $i^{th}$  CAV's rear bumper, and the length of the  $i^{th}$  vehicle, respectively. A fixed time headway gap spacing policy, which can improve the string stability and safety [9], is considered as follows

$$d_i^*(t) = T_i v_i(t) + d_i^0, (3)$$

where  $T_i$  is the time gap, and  $d_i^0$  is the standstill distance. The difference between the gap and its desired value is defined as  $\Delta d_i(t) = d_i(t) - d_i^*(t)$ . Hence,  $\Delta \dot{d}_i$  turns into  $\Delta \dot{d}_i(t) = v_{i-1}(t) - v_i(t) - T_i \, a_i(t)$ , where  $a_i$  denotes the acceleration of the  $i^{th}$  vehicle. By taking the driveline dynamics  $\tau_i$  into account, the derivative of the acceleration for vehicle i is  $\dot{a}_i(t) = -\frac{1}{\tau_i} a_i(t) + \frac{1}{\tau_i} u_i^a(t)$ , where  $u_i^a(t)$  acts as the vehicle's acceleration input.

Considering  $x_i(t) = [\Delta d_i(t) \ y_i(t) \ \theta_i(t) \ v_i(t) \ a_i(t)]^T$ , the state-space representation for CAV<sub>i</sub> becomes

For the leader vehicle (i=0), the term  $v_{i-1}(t)$  in (4) is replaced by its desired speed trajectory. Using forward-time approximation for the first-order derivative, (4) can be expressed in discrete time as

$$x_i(k+1) = (I + t_s A_i) x_i(k) + t_s B_i u_i(k) + t_s C_i v_{i-1}(k),$$
(5)

where I is the identity matrix and  $t_s$  is the sampling time. Next, we will introduce the preliminaries of SMPC which will be used to handle the uncertainties of HVs' maneuvers.

## A. Scenario-based model predictive control

SMPC uses a tree of discrete scenarios to describe the system uncertainties. Any branch stemming from a node represents a scenario of an unknown, uncertain influence (e.g., from a disturbance or model error) [6]. The scenario-based optimal control problem for an uncertain system at time step k can be formulated as follows

$$\min_{x^{j}, u^{j}} \sum_{j=1}^{S} p^{j} \left[ \sum_{i=0}^{N-1} \ell\left(x^{j}(i|k), u^{j}(i|k)\right) + V_{N}\left(x^{j}(N|k)\right) \right]$$

s.t. 
$$x^{j}(i+1|k) = f(x^{j}(i|k), u^{j}(i|k), \hat{y}^{j}(i|k)),$$
 (6a)

$$(x^j(i|k), u^j(i|k)) \in \mathcal{X} \times \mathcal{U},$$
 (6b)

$$x^j(0|k) = x(k), (6c)$$

$$u^{j}(i|k) = u^{l}(i|k) \text{ if } x^{p(j)}(i|k) = x^{p(l)}(i|k),$$
 (6d)

where  $p^j$  is the probability of the j-th scenario;  $\ell\left(x^j(i|k),u^j(i|k)\right)$  and  $V_N\left(x^j(N|k)\right)$  are the stage cost and terminal cost for the j-th scenario, respectively; N is the prediction horizon,  $\hat{\mathbf{y}}^j(i|k)$  is the uncertainty realization considered at time instant i for the j-th scenario; (6d) enforces a non-anticipativity constraint, which represents the fact that each control input that branches from the same parent node must be equal  $(x^{p(j)}(i|k))$  is the parent state of  $x^j(i+1|k)$ . The non-anticipativity constraint is crucial in order to accurately model the real-time decision problem such that the control inputs do not anticipate the future (i.e., decisions cannot realize the uncertainty). The solution to this optimization problem is used to generate the control law, presented as

$$\kappa\left(x(k)\right) = u^{\star}(0|k). \tag{7}$$

To reduce computational complexity, we utilize a robust horizon  $N_r < N$  defined in [6]. This robust horizon stops the branching of the scenario tree up to a certain stage, and the uncertainty is assumed to be constant thereafter. Consequently, assuming the number of scenarios s at each node of a stage is constant, the total number of scenarios s can be represented by  $s = s^{N_r}$ . For scenario generation, several methods of scenario generation have been proposed in the literature, including Monte Carlo sampling methods [10], moment matching methods [11], [12], and even machine learning techniques [13], [14]. The objective of scenario tree construction is to accurately approximate (6) with a relatively small number of scenarios.

# III. SYSTEM MODEL IN THE MIXED LOGICAL DYNAMICAL FORM

The discrete hybrid automata (DHA) [15] unit is used to describe each CAV dynamics and constraints together with its four operating modes, namely free following (FF), danger (D), braking (B), and lane change (LC). In the control unit, the DHA is transformed into Mixed Logical Dynamical (MLD) form and then used to solve the scenario-based hybrid MPC problem. The optimal control input is applied to the system actuator(s), and the predictive speed trajectory is shared with follower vehicles through V2V communication. In the remainder of this section, additional details are provided on how to represent CAV equations in the MLD form.

The constraints on the system include

$$a_i^{min} \le a_i(k) \le a_i^{max},\tag{8a}$$

$$u_i^{min} \le u_i^a(k) \le u_i^{max},\tag{8b}$$

$$v_i(k) \le v_{max},$$
 (8c)

$$d_i(k) > 0. (8d)$$

In our CACC design, the following four operating modes are considered with the transition diagram shown in Fig. 1:

- free-following mode, where each CAV attempts to keep a desired distance from its CAV predecessors;
- braking mode, where CAV attempts to slightly increase its headway and reduce its speed to avoid a possible accident;
- 3) danger mode, where an HV is changing (or has changed) its lane and is moving in front of the CAV (in this case, the CAV right behind the HV adjusts its headway according to the preceding HV's location;
- 4) lane-change mode, in which the CAV tries to overtake an HV and reduces the distance between itself and its preceding CAV.

Four binary auxiliary variables representing system events are defined as follows

 $\delta_i^N(k) = 1 \iff$  free-following event is activated;

 $\delta_i^D(k) = 1 \iff$  danger event is activated;

 $\delta_i^B(k) = 1 \iff \text{braking event is activated};$ 

 $\delta_i^L(k) = 1 \iff$  lane-change event is activated.

1) Braking event: The speed difference between  $CAV_i$  and its predecessor is efined as  $\Delta v_i(k) = v_{i-1}(k) - v_i(k)$ . As long as  $\Delta v_i(k)$  is greater than a safety threshold  $v_i^s < 0$ , the vehicle operates in the free-following mode. However, if  $\Delta v_i(k)$  goes below the safety threshold, the  $i^{th}$  vehicle enters braking mode. Therefore,

$$\Delta v_i(k) \le v_i^s \iff \delta_i^B = 1. \tag{9}$$

To preserve safety, when a vehicle's braking event is activated ( $\delta_i^B=1$ ), its target velocity will change from  $v_{i-1}$  to a smaller value  $v_{i-1}-v_i^b$  while its target headway increases by  $v_i^b\,T_i$ , where  $v_i^b$  is a design parameter.

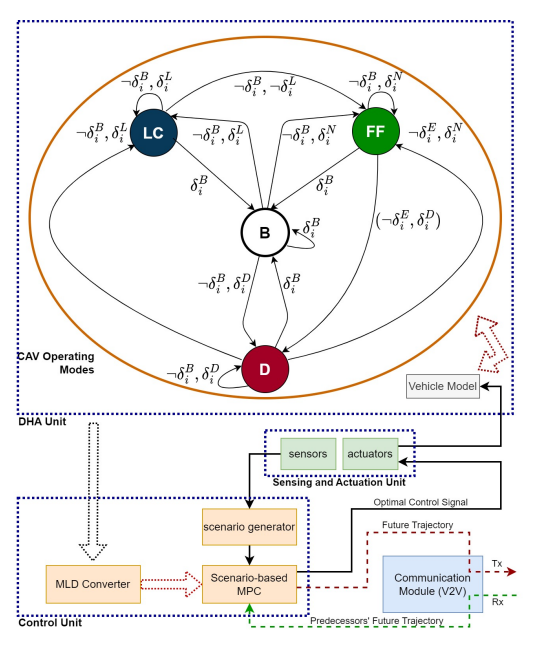


Fig. 1: Diagram of the proposed scenario-based hybrid MPC design for CACC. The scenario generator block uses the closest HV's location to generate the scenario tree. The control unit translates the CAV's model into MLD and employs a scenario-based hybrid MPC to find the optimal control input. Each CAV uses the future profiles of its predecessors, which are received through V2V communication, for finding its optimal control actions.

The representation of (9) in the MLD form is as follows:

$$\Delta v_i(k) - v_i^s \le M_i^f [1 - \delta_i^B],$$
  

$$\Delta v_i(k) - v_i^s \ge \varepsilon + \delta_i^B [m_i^f - \varepsilon],$$
(10)

where  $\varepsilon$  is the machine precision, and  $m_i^f$  and  $M_i^f$  denote lower and upper bounds on  $\Delta v_i(k) - \underline{v}^f$ , respectively.

2) Danger event: When an HV starts to switch lane and moves in front of a CAV (which can be detected through the CAV sensors and cameras), a danger event occurs. In this case, the CAV in danger mode should adjust its headway based on the HV position instead of the preceding CAV's position. So, the auxiliary binary variable  $\delta_i^D(k)$  is defined such that

$$y_{i+1}^h(k) - y_i(k) \le y_i^{th} \to \delta_i^D(k) = 1,$$
 (11)

where  $y_i^{th}$  is the danger event threshold. Danger event for  $CAV_i$  occurs for one of the following two reasons:

- a) the CAV is in free-following mode, and the adjacent HV begins changing its lane and entering the CAVs' platoon.
- b)  $CAV_i$  is in the free-following mode, and  $CAV_{i-1}$  is doing a lane change; hence, the  $i^{th}$  CAV's immediate predecessor in the lane becomes an HV. In this case,  $CAV_{i-1}$  announces its lane-change decision as a binary flag  $f_{i-1}^{LC}$  to its follower CAV through communication. Hence, the following statement should hold true

$$f_{i-1}^{LC}(k) = 1 \to \delta_i^D(k) = 1.$$

Remark 1: When the danger event occurs, the CAV adjusts its velocity and headway based on the HV that causes the danger. Hence, the CAV's distance from its preceding vehicle (can be either a CAV or an HV)  $d_i(k)$  can be redefined as

$$d_i(k) = (1 - \delta_i^D(k)) x_{i-1}(k) + \delta_i^D(k) x_i^h(k) - x_i(k) - l_i^v,$$
 and  $\Delta d_i(k)$  changes accordingly.

3) Lane-change event: When a CAV is in the danger mode, and its longitudinal distance from its preceding CAV exceeds a predefined threshold, the CAV should perform a lane change to be able to reach its desired spacing policy, and hence

$$\delta_i^L(k) = 1 \iff x_{i-1}(k) - x_i(k) - l_i^v - (T_i + \alpha_i) v_i(k) \ge 0,$$

where  $\alpha_i > 0$  is the threshold mentioned above. Whenever the lane-change mode activates, the lateral reference for the CAV changes to the desired lateral location in the adjacent lane.

To ensure a collision-free lane change, CAVs should also consider HVs in the target lane. To this aim, the lane-change mode for a CAV should not activate unless there is no vehicle in the target lane behind the CAV or the CAV is able to preserve a minimum distance from that vehicle during the lane-change maneuver; the latter for  $CAV_i$  is addressed using the following constraint

$$x_i(k) - x_{i+1}^h(k) - l_{i+1}^h(k) - \beta_i v_{i+1}^h \ge 0,$$

where  $\beta_i$  represents the minimum allowed time gap from the rear HV in the target lane,  $x_{i+1}^h$ ,  $l_{i+1}^h$  and  $v_{i+1}^h$  are location, length, and velocity of the HV in the CAV's target lane, respectively. It is noted that whenever the lane-change mode activates for  $CAV_i$ , danger event for that vehicle terminates.

4) Free-following event: Free-following event for i<sup>th</sup> CAV occurs when none of the three other events are activated for the CAV.

Considering the aforementioned events changes the difference equations in (5) to the following form

$$x_{i}(k+1) = (I + t_{s} A_{i}) x_{i}(k) + t_{s} B_{i} u_{i}(k) + t_{s} C_{i} [(1 - \delta_{i}^{D}(k)) v_{i-1}(k) + \delta_{i}^{D}(k) v_{i}^{h}(k)], \quad (12)$$

where  $v_i^h(k)$  is the velocity of the HV that activates the danger event for the  $i^{th}$  CAV.

# IV. SCENARIO-BASED MPC DESIGN FOR CACC

The proposed controller design approach for CACC is shown in Fig. 1. CAVs leverage an m look-ahead communication topology, and each CAV shares its predictive speed trajectory with a number of its followers. The scenario tree construction for the SMPC depends on the description of uncertainties. In this work, we assume that the lateral velocity of the HVs comes from a Gaussian distribution. The distribution varies based on the relative location of the HV and the CAV. For example, in Fig. 2, four clusters are considered, and a specific distribution over the clusters is used to model the HV's uncertain lateral behavior. In general, the distributions

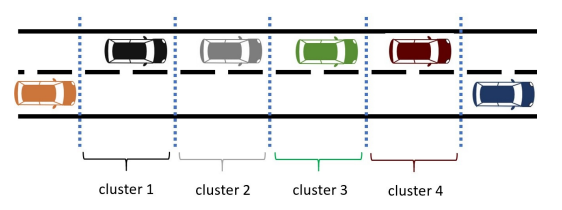


Fig. 2: The representation of the clusters considered for the HV's behavior. Orange and blue vehicles represent CAVs while the rest represent HVs.

can be learned using real data of HVs' lateral behavior. It is noted that, if the HV does not belong to any of the clusters, its lateral velocity is assumed to be zero.

In particular, the distribution for cluster j is considered as a Gaussian distribution  $\mathcal{N}(\mu_j,\sigma_j^2)$  which can be discretized and used to create the scenario tree. In this paper, the distribution corresponding to cluster j is discretized into three levels, namely,  $\mu_j - \sigma_j$ ,  $\mu_j$  and  $\mu_j + \sigma_j$  with the probabilities of  $0.159\,,0.682\,,0.159$ , respectively. This means that when branching a node, three new nodes are added to the tree. The model predictive problem constructed upon the scenario tree for  $CAV_i$  is formulated as follows

$$\begin{split} \min_{\mathbf{u}_{i}^{j}, \mathbf{z}_{i}^{j}} \sum_{j=1}^{S} P^{j} \left[ \sum_{k=0}^{N-1} \left( (x_{i}^{j}(k) - R_{i}^{j})^{T} \, Q_{i} \, (x_{i}^{j}(k) - R_{i}^{j}) \right) \right] \\ + \sum_{n=i-m}^{i-1} \left[ c_{i,n}^{d} \left( x_{n}(k) - x_{i}^{j}(k) - \sum_{r=n+1}^{i} (d_{r}^{*}(k) + l_{r}^{v}) \right. \\ \left. - \delta_{i}^{B}(k) \, v_{i}^{b} T_{i} \right)^{2} \right. \\ + c_{i,n}^{v} \left( v_{n}(k) - v_{i}^{j}(k) - \delta_{i}^{B}(k) \, v_{i}^{b} \right)^{2} \right] + c_{i}^{E} \right], \\ \text{subject to:} \quad \text{MLD system equations,} \\ u_{i}^{j}(k) = u_{i}^{l}(k) \text{ if } x_{i}^{p(j)}(k) = x_{i}^{p(l)}(k), \end{split}$$

where the superscript j is used to distinguish the system states and inputs for different scenarios,  $\mathbf{u}_i^j$  and  $\mathbf{z}_i^j$  are the system inputs and the vector of auxiliary variables from k=0 to k=N-1, respectively. The positive coefficients  $c_{i,j}^d>0$  and  $c_{i,j}^v$  penalize the distance and speed difference between  $CAV_i$  and  $CAV_n$  (n<i), the terms  $\delta_i^B(k)\,v_i^b$  and  $\delta_i^B(k)\,v_i^bT_i$  are used to reduce the desired velocity and increase the desired distance in braking mode, respectively, and m denotes the number of predecessors sharing information with the  $i^{th}$  CAV. In (13), each vehicle tends to achieve the desired distances from its m predecessors while adjusting its velocity based on the predecessors' velocities. It is noted that when m>i (number of predecessors is less than m),  $CAV_i$  replaces m with i in (13).

### V. SIMULATION RESULTS AND DISCUSSION

For the CACC problem, the performance of the proposed scenario-based MPC is evaluated in a mixed-autonomy traffic system including two lanes, where HVs may perform lane change and merge into the CAVs' platoon. Parameters used in the simulation study can be found in [5]. In the MPC problem (13), the vector  $R_i$  is chosen as follows

$$R_{i} = \begin{bmatrix} 0.7 \, \delta_{i}^{D}(k) \, T_{i} \, v_{i}(0) + \delta_{i}^{B}(k) \, v_{i}^{b} T_{i} & 0 & y_{i}^{ref}(k) \\ (1 - \delta_{i}^{D}(k)) \, v_{i-1}(k) - \delta_{i}^{D}(k) \, v_{i}^{h}(k) + \delta_{i}^{B}(k) \, v_{i}^{b} & 0 \end{bmatrix}^{T}.$$

Such selection for  $R_i$  implies that if a danger event does not occur (or will not occur within the prediction horizon),  $CAV_i$  only considers its m predecessor CAVs' information for adjusting its speed. However, according to Remark 1, the activation of the danger event results in taking the distance from the adjacent HV and the HV's velocity into account in finding the optimal control input. It is noted that  $CAV_i$  uses  $T_i(v_i(k) + 0.7 v_i(0)) + d_i^0$  as its desired distance from the adjacent HV in danger mode. In addition, the terms  $\delta_i^B(k) v_i^b$ and  $\delta_i^B(k) v_i^b T_i$  are used to reduce the desired velocity and increase the desired distance in braking mode, respectively. The parameter  $v_i^b$  is considered as  $0.01 v_i(t)$ . In this study, it is assumed that each HV's lateral velocity comes from the following Gaussian distributions:  $\mathcal{N}(0, 0.25^2)$  for Cluster 1,  $\mathcal{N}(0,0.5^2)$  for Cluster 2,  $\mathcal{N}(0,1^2)$  for Cluster 3,  $\mathcal{N}(0,2^2)$ for Cluster 4. The underlying mixed-integer optimization problems are solved using CVXPY package, and Gurobi solver in Python. It is also assumed that HVs may perform lane change only once during the simulation study. The results are also compared against the previously developed discrete hybrid stochastic MPC design (DHSA MPC) [5]. In our experiments, a platoon of seven CAVs is considered while three HVs are assumed to move initially in the adjacent lane next to the CAVs. A graphical representation of the simulation results at eight different moments is illustrated in Fig. 3, and the location of the vehicles at the beginning of the simulation is shown in the first subplot. The subplots showing  $\Delta d_i$ ,  $y_i$ ,  $v_i$ , and  $a_i$  are given in Fig. 4 for the scenario-based MPC, and Fig. 5 for DHSA MPC. Initially, the velocity of both  $HV_0$  and  $HV_1$  is  $26 \, m/s$  while the velocity of  $HV_2$ is  $20 \, m/s$ .  $HV_0$  performs a lane change at  $t = 9 \, s$  while keeping the same speed. However, when  $HV_1$  changes its lane at  $t = 12 \, s$ , it also reduces its speed to  $23 \, m/s$ .  $HV_3$ does not perform a lane change. The initial velocity for all CAVs is  $20 \, m/s$  while their desired velocity is  $29 \, m/s$ .

At the beginning of the simulation, all CAVs operate in free-following mode (first subplot at Fig. 3). In between t = 5s - t = 10s,  $CAV_1$  and  $CAV_6$  slightly deviate from the desired policy due to considering possible HVs' lane-change maneuver through the decision tree. At around t = 9.3s,  $HV_0$  initiates the lane-change maneuver, which results in  $CAV_1$  lane change at around t = 9.5s as the reaction to such an event.  $CAV_2$ , however, does not immediately perform a lane change due to possible danger because of the presence of another HV in the target lane, and waits until around t = 12.6s to change its lane. This results in a noticeable deviation from the desired spacing and velocity policy during t = 9.5 - 12.6s. At t = 12.3s,  $HV_1$  starts its lane-change maneuver, causing  $CAV_3$  to slightly deviate from its desired spacing and velocity policy.  $CAV_3$  reacts quickly to this event and enters lane-change mode. Other

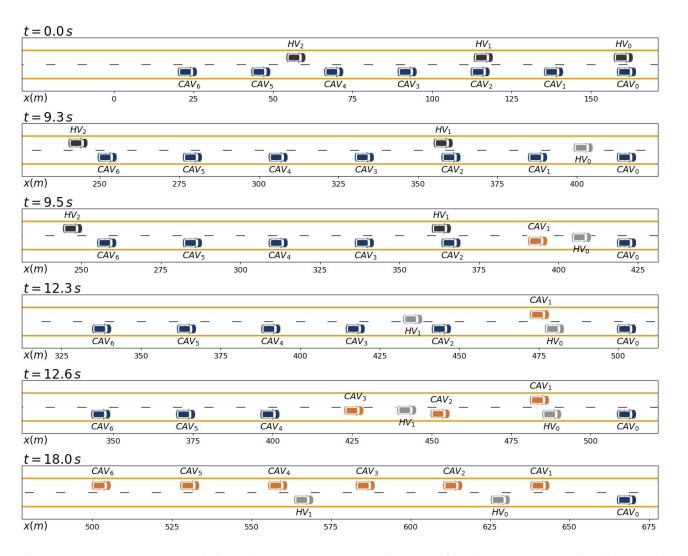


Fig. 3: The graphical representation of the scenario-based MPC performance for a fleet including 7 CAVs and 3 HVs where  $\alpha_i=0.25\,s$ . HVs in the top lane are shown in black, while after beginning a lane change, their color is changed to gray. CAVs are shown using blue color, and after their lane-change mode activates, their color is changed to orange.

CAVs in the platoon  $(CAV_4 - CAV_7)$  do the same thing one after another to avoid their distance from their predecessor increasing. As shown in Fig. 4, after t=18s all CAVs

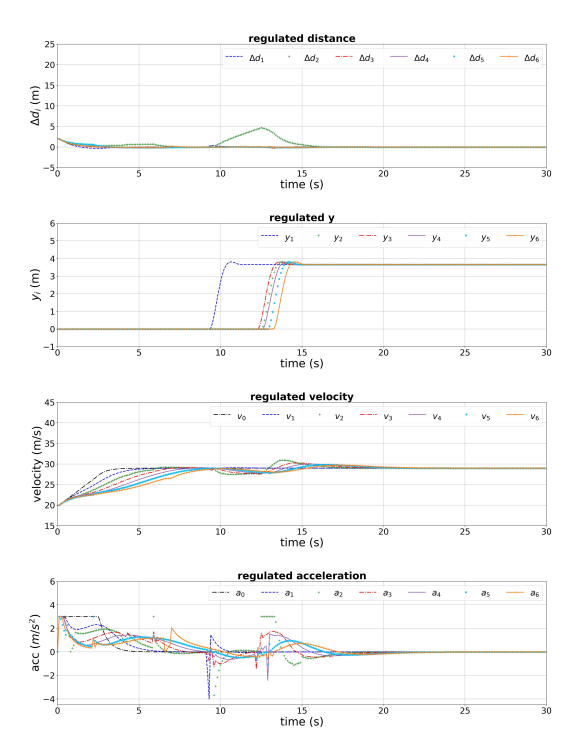


Fig. 4: Performance of the CAVs employing the scenario-based MPC scheme for a fleet including 7 CAVs and 3 HVs. are able to achieve their desired behavior. Considering the same initial conditions, Fig. 5 shows the simulation results when using DHSA MPC. The DHSA MPC behavior shows significant deviations from the desired spacing and velocity policies, and noticeable variations in CAVs' acceleration

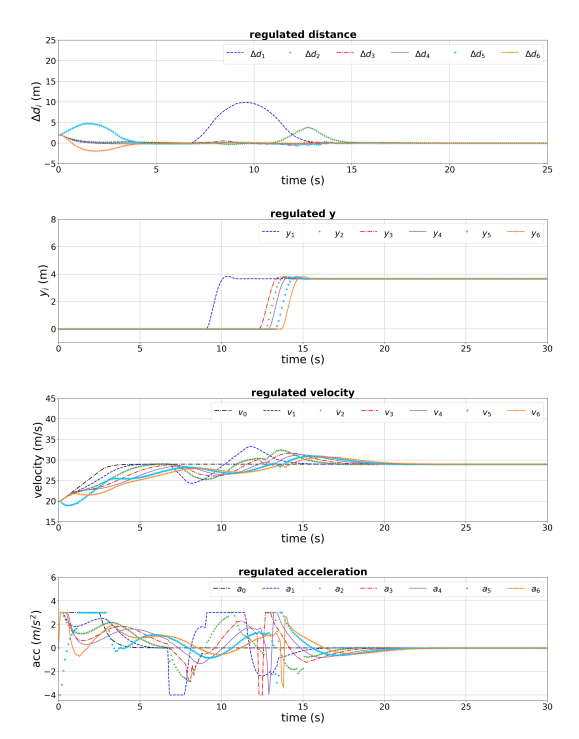


Fig. 5: Performance of the CAVs employing the DHSA MPC scheme for a fleet including 7 CAVs and 3 HVs.

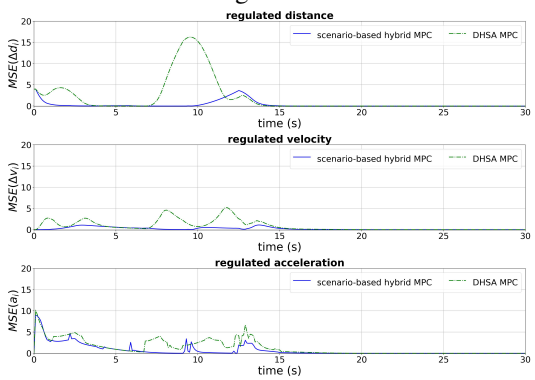


Fig. 6: Comparing the mean squared error for two control approaches: scenario-based MPC and DHSA MPC.

profiles, compared with the scenario-based approach. The main reason behind such differences in the closed-loop behaviors under DHSA MPC and the proposed scenario-based MPC is as follows. The DHSA MPC controller chooses a single realization of uncertainties that yields the lowest cost to the controller and optimizes the control input for that specific trajectory; on the other hand, the scenario-based MPC controller optimizes the behavior of CAVs over multiple realizations of uncertainties that are considered in the scenario tree. The Mean Squared Error (MSE) measure is also used to compare the two aforementioned control approaches. The MSE of  $\Delta d_i$ ,  $v_i$ , and  $a_i$  are considered for all CAVs, and the values at each time step are plotted in Fig. 6, which shows that scenario-based MPC provided significant improvements compared to DHSA MPC.

### VI. CONCLUDING REMARKS

In this paper, a scenario-based hybrid MPC design was developed for cooperative adaptive cruise control to deal

with uncertainties in the environment. In particular, the uncertainty that arises from unpredictable human-driven vehicles' maneuvers in a mixed-autonomy traffic environment was considered. Several operating modes, namely free following, braking, danger, and lane change, for each CAV were considered to adapt the CAV's behavior based on the HVs maneuvers. Each CAV's operating mode was chosen based on the predictive information it receives from its predecessors and the anticipated behaviors of surrounding HVs. Employing scenario-based MPC design improved the robustness of the controller against the uncertainties in the environment.

#### REFERENCES

- J. Ni, J. Han, and F. Dong, "Multivehicle cooperative lane change control strategy for intelligent connected vehicle," *Journal of Advanced Transportation*, vol. 2020, 2020.
- [2] T. Peng, L. Su, R. Zhang, Z. Guan, H. Zhao, Z. Qiu, C. Zong, and H. Xu, "A new safe lane-change trajectory model and collision avoidance control method for automatic driving vehicles," *Expert Systems with Applications*, vol. 141, p. 112953, 2020.
- [3] S. Liu, H. Su, Y. Zhao, K. Zeng, and K. Zheng, "Lane change scheduling for autonomous vehicle: A prediction-and-search framework," in Proceedings of the 27th ACM SIGKDD Conference on Knowledge Discovery & Data Mining, 2021, pp. 3343–3353.
- [4] Z. Zhang, L. Zhang, J. Deng, M. Wang, Z. Wang, and D. Cao, "An enabling trajectory planning scheme for lane change collision avoidance on highways," *IEEE Transactions on Intelligent Vehicles*, 2021.
- [5] S. Mosharafian and J. M. Velni, "Cooperative adaptive cruise control in a mixed-autonomy traffic system: A hybrid stochastic predictive approach incorporating lane change," *IEEE Transactions on Vehicular Technology*, 2022.
- [6] S. Lucia, T. Finkler, and S. Engell, "Multi-stage nonlinear model predictive control applied to a semi-batch polymerization reactor under uncertainty," *Journal of Process Control*, vol. 23, no. 9, pp. 1306–1319, 2013
- [7] Y. Bao, K. J. Chan, A. Mesbah, and J. M. Velni, "Learning-based adaptive-scenario-tree model predictive control with improved probabilistic safety using robust bayesian neural networks," *International Journal of Robust and Nonlinear Control*, vol. 33, no. 5, pp. 3312– 3333, 2023.
- [8] S. Mosharafian and J. M. Velni, "A hybrid stochastic model predictive design approach for cooperative adaptive cruise control in connected vehicle applications," *Control Engineering Practice*, vol. 130, p. 105383, 2023.
- [9] G. J. Naus, R. P. Vugts, J. Ploeg, M. J. van De Molengraft, and M. Steinbuch, "String-stable cacc design and experimental validation: A frequency-domain approach," *IEEE Transactions on vehicular technology*, vol. 59, no. 9, pp. 4268–4279, 2010.
- [10] A. Shapiro, "Monte carlo sampling methods," Handbooks in operations research and management science, vol. 10, pp. 353–425, 2003.
- [11] K. Høyland, M. Kaut, and S. W. Wallace, "A heuristic for moment-matching scenario generation," *Computational optimization and applications*, vol. 24, no. 2, pp. 169–185, 2003.
- [12] Y. Bao, K. J. Chan, A. Mesbah, and J. M. Velni, "Learning-based adaptive-scenario-tree model predictive control with probabilistic safety guarantees using bayesian neural networks," in 2022 American Control Conference (ACC). IEEE, 2022, pp. 3260–3265.
- [13] B. Defourny, "Machine learning solution methods for multistage stochastic programming," PhD diss., University of Liege. https://www. lehigh. edu/defourny/PhDthesis\_B\_Defourny, pdf, 2010.
- [14] Y. Bao, H. S. Abbas, and J. Mohammadpour Velni, "A learning-and scenario-based mpc design for nonlinear systems in lpv framework with safety and stability guarantees," *International Journal of Control*, pp. 1–20, 2023.
- [15] F. D. Torrisi and A. Bemporad, "Hysdel-a tool for generating computational hybrid models for analysis and synthesis problems," *IEEE transactions on control systems technology*, vol. 12, no. 2, pp. 235–249, 2004.